Shift-Variance Analysis of the Q-shift Dual-Tree Complex Wavelet Transform

Marzieh Rahmani Moghadam

Submitted to the
Institute of Graduate Studies and Research
in partial fulfillment of the requirements for the Degree of

Master of Science
in
Electrical and Electronic Engineering

Eastern Mediterranean University
February 2014
Gazimağusa, North Cyprus

Approval of the Institute of Graduate Studies and Research

Prof. Dr. Elvan Yılmaz
Director

I certify that this thesis satisfies the requirements as a thesis for the degree of Master of Science in Electrical and Electronic Engineering.

Prof. Dr. Aykut Hocanın
Chair, Department of Electrical and Electronic Engineering

We certify that we have read this thesis and that in our opinion it is fully adequate in scope and quality as a thesis for the degree of Master of Science in Electrical and Electronic Engineering.

Prof. Dr. Runyi Yu
Supervisor

Examining Committee

1. Prof. Dr. Aykut Hocanın _____

2. Prof. Dr. Hüseyin Özkaramanlı _____

3. Prof. Dr. Runyi Yu _____

ABSTRACT

We analyze the shift-variance of the Dual-Tree Complex Wavelet Transform (DT-CWT) in this thesis. In our study, the DT-CWT is treated as a generalized sampling process. The analysis of shift-variance is performed in terms of two quantities: the shift-variance level (SVL) and the shift-variance measure (SVM). The SVL describes the amount of distance between the system and the set of systems which are so-called μ-shift-invariant (specifying how the system has to respond to the shifted input signal). The SVM is equal to the SVL divided by two times of the system norm.

We obtain the SVL and the SVM for the DT-CWT and the scaling function for Kingsbury's Q-shift filters of length 8, 12, 18, and 22. We observe that the shift-variance varies as the Q-shift filter length changes. When the length of the filter increases, the SVM becomes closer to the zero. This means that DT-CWT is almost shift-invariance. For better illustrating the shift-invariance property, we consider an input signal and its shifted version to compare the outputs corresponding to the DT-CWT and the scaling function.

Keywords: Dual-tree complex wavelet transforms, scaling function, shift-variance level, shift-variance measure, Q-shift filters.

ÖZ

Bu tez çalışmasında Çift Ağaç Karmaşık Dalgacık Dönüşümü'nün (ÇA-KDD) değişen dağılımı incelenmektedir. Tez çalışmamızda ÇA-KDD genelleştirilmiş örneklendirme süreci olarak işlem görmüştür. Değişen dağılım analizi, değişen dağılım düzeyi (DDD) ve değişen dağılım ölçütü (DDÖ) olmak üzere iki değer aracılığıyla yapılmıştır. DDD, sistem ve μ-değişimden bağımsız (sistemin değişime uğramış giriş sinyaline göre nasıl tepki göstermesini belirleyen) olarak adlandırılan bir dizi sistemler arasındaki uzaklık miktarını tanımlamaktadır. DDÖ ise iki kez sistem modeline bölünmüş olan DDD'ye eşittir.

ÇA-KDD için DDD ve DDÖ ve aynı zamanda Kingsbury'nin 8, 12, 18 ve 22 uzunluğunda olan Q-değişkenli filtrelerinin ölçeklendirme fonksiyonları elde edilmiş ve karşılaştırılmıştır. Karşılaştırma sonucunda Q-değişkenli filtrelerin uzunluk değişimlerine paralel olarak değişen dağılımının çeşitlilik gösterdiği gözlemlenmiştir. Filtrenin uzunluğunun artırılmasına paralel olarak, DDÖ değerinin sıfıra yakın bir değer aldığı ve ÇA-KDD'nın hemen hemen değişimden bağımsız olduğu ortaya çıkmıştır. Değişimden bağımsız olma özelliğini daha iyi örneklendirmek amacıyla giriş sinyali ve aynı sinyalin değişime uğramış versiyonunun ÇA-KDD ve ölçekleme işlemi ile ilgili çıktılarının karşılaştırılması dikkate alınmıştır.

Anahtar Kelimeler: Çift Ağaç Karmaşık Dalgacık Dönüşümleri, ölçekleme işlevi, değişen dağılım düzeyi, değişen dağılım ölçütü, Q-değişkenli filtreler

DEDICATION

To

my lovely parents, Mohamad Hassan and Fatemeh;

my sweetie sister, Mahboobeh;

my beloved husband Seyedvahid Amirinezhad

ACKNOWLEDGMENTS

I wish to express my sincere gratitude to my supervisor Prof. Dr. Runyi Yu for his interest and continuous support in the preparation of this thesis.

I would like to thank Prof. Nick Kingsbury for providing the MATLAB codes which generate the Q-shift filters.

Finally, it is my pleasure to acknowledge a number of my friends who have supported me morally.

TABLE OF CONTENTS

LIST OF TABLES

LIST OF FIGURES

LIST OF SYMBOLS/ABBREVIATIONS

$\mathcal{B}$	Defining band
c_k	Scaling function coefficient
$d_{j,k}$	Wavelet coefficient
$\mathcal{D}^{\tau}$	Continuous-time shift operator
$\mathcal{D}_{\mathcal{B}}^{\alpha}$	Discrete-time shift operator
g_0	Low-pass filter in upper FB
g_1	High-pass filter in upper FB
h_0	Low-pass filter
h_1	High-pass filter
$\mathcal{H}$	Hilbert transform
H_0	Low-pass filter in Fourier domain
$\mathbf{H}_0$	Vector of H_0
H_1	High-pass filter in Fourier Domain
$\mathbb{R}$	Set of real numbers
$\mathcal{S}$	System
$\mathbb{Z}$	Set of integer numbers
$\mathcal{K}_{\tau,\mathcal{B}}$	Commutator of system
$\kappa(\mathcal{S})$	Shift-variance level
$\nu(\mathcal{S})$	Shift-variance measure
τ	Delay
ϕ	Scaling function in time domain

Φ	Scaling function in Fourier domain
ψ	Wavelet Transform in time domain
$\psi_c(t)$	Complex wavelet
$\psi_g(t)$	Real part of DT-CWT
$\psi_h(t)$	Imaginary part of DT-CWT
$\psi_i(t)$	Imaginary part of wavelet
$\psi_r(t)$	Real part of wavelet
Ψ	Wavelet Transform in Fourier domain
$\mathbb{C}$WT	Complex Wavelet Transform
DT-CWT	Dual-Tree Complex wavelet transform
DWT	Discrete Wavelet Transform
FIR	Finite Impulse Response
PR	Perfect reconstruction
sup	Supremum
SVL	Shift-variance level
SVM	Shift-variance measure

Chapter 1

INTRODUCTION

1.1 Introduction

The discrete wavelet transform may be used as a signal-processing tool for visualization and analysis of nonstationary, time-sampled waveforms. The highly desirable property of shift invariance can be obtained at the cost of a moderate increase in computational complexity, and accepting a least-squares inverse (pseudoinverse) in place of a true inverse. The shift-invariance is so prominence in many signal processing applications. Owning to this, a wide range of attempts has been dedicated to seeking discrete-time transforms that can have good shift-invariance. In this regard, several different discrete-time transforms have been recommended such as the wavelet packet decomposition [1], the dual-tree complex wavelet transform [2], [3], the pre-processing complex wavelet transforms [4], the post Hilbert transform of the discrete wavelet transform (DWT) [5], and the shiftable DWT [6].

Although a number of transforms have been proposed for satisfying shift-invariance property, there were not any criteria to quantify the shift-variance for them. In other words, the existence of some quantities was essential to judge shift-invariance property between these transforms. Kingsbury [2] proposed quantification of shift dependence as the ratio of two energy: the energy of transfer functions with aliasing component and the energy of transform which is non-aliasing. To quantifying shift-

variance Aach and Führ [7] analyzed the effects of the linear periodically shift variant system on deterministic and statistical signals within a unified framework by quantifying shift variance of operators. Furthermore Yu [8] he proposed two parameters (i.e. SVL and SVM) to analyze shift-variance. Indeed, the shift-variance is presented absolutely by SVL and relatively by SVM. Moreover he applied these two quantities to some complex transforms such as DWT and short-time Fourier transform (STFT). He also proposed SVM for multirate systems [9].

In this study, we consider the dual-tree complex wavelet transform (DT-CWT) [2, 3] as a discrete-time transform. The DT-CWT, proposed by Kingsbury [2] enhances the DWT by adding significant properties such as approximate shift-invariance and directionally selectivity in two and higher dimensions.

It must be mentioned that the structure of dual-tree put additional demands on the filters that are used in the wavelet transform, in order to accomplish optimal shift-invariance. An effective approach was proposed by Kingsbury [10] for developing the optimality of the Q-shift filters of the DT-CWT. In particular, these designs are useful in image processing since the resulting complex wavelets and the scaling functions satisfy the linear-phase property.

This thesis concentrates on analyzing shift-variance on DT-CWT and the scaling function with the Q-shift filters by quantifying their shift-variance. For this aim, the different lengths of Q-shift filters such as 8, 12, 18, and 22 are considered. It can be observed that the DT-CWT with the Q-shift filters has indeed good shift-invariance, and the shift-invariance improved as the length of the filters. For example, the SVM is very small (8.6%) for the DT- CWT with the Q-shift filters of length 22 in the

defining band. To illustrate the shift-invariance we consider an input signal and its shifted version to compare the outputs corresponding to the DT-CWT and the scaling function with the Q-shift filter.

1.2 Organization

This thesis is organized in five chapters:

Chapter 1 includes a brief review of previous literature works on shift-invariance. The common problems of discrete-time transforms are mentioned. In Chapter 2, the Discrete Wavelet Transform, the Complex Wavelet Transform ($\mathbb{C}$WT), and the DT-CWT are briefly introduced. The structure and filters designing of DT-CWT are described. The design of Kingsbury's Q-shift filters is also explained in this chapter.

Chapter 3 starts with mathematical description of the generalized sampling process. Then, we describe the idea of the μ-shift-invariance. Moreover, we present the SVL and SVM, and the formulas of these parameters are analytically expressed in more detail. By computing the SVL and SVM, the analysis of shift-variance for the DT-CWT and the scaling function will be done. The Q-shift filters are used in analyzing the shift-invariance properties of the DT-CWT. We then present the analysis of the shift-variance for the DT-CWT and the scaling function with the Q-shift filters of different length. Finally, Chapter 5 concludes the thesis.

Chapter 2

DUAL-TREE COMPLEX WAVELET TRANSFORMS

In this chapter, wavelet transform, Discrete Wavelet Transform (DWT), and Complex Wavelet Transform ($\mathbb{C}$WT) will be introduced in brief. Then Dual-Tree Complex Wavelet Transform (DT-CWT) and its features will be stated. Furthermore the design of Kingsbury's Q-shift filters will be explained.

2.1 Wavelet Transforms

Wavelet can be considered as a small wave and it has oscillating function. The energy of wavelet focuses on time in order to provide the ability of analysis of transient, nonstationary, or time-varying phenomena. Furthermore, the ability of simultaneous time and frequency analysis through flexible mathematical foundation are allowed by wavelet. Also Wavelet has utilized an impressive reputation as a tool for signal, image, and video processing.

If we expand and shift a real-valued band pass and fundamental wavelet $\psi(t)$ (i.e. generating wavelet or mother wavelet), the different forms of wavelets can be developed as follows:

$$\psi_{j,k}(t) = 2^{j/2}\psi(2^j t - k), \qquad j,k \in \mathbb{Z} \tag{2.1}$$

where $\mathbb{Z}$ is the set of all integers and the amount of norm independent of scale j is held by the factor $2^{j/2}$. For developing the wavelet expansion (2.1), it is crucial to use the idea of an expansion set or basis set. Therefore, the idea of scale should be stated for this aim.

Scaling is a kind of mathematical operations such that a signal can be either expanded or compressed. In the wavelet analysis, the *scale* parameter is identical to the scale employed in maps. High scales are associated with a non-detailed global view and low scales are related to a detailed view. Particularly, in frequency domain, it can be possible to say that low frequencies are related to global information of a signal though high frequencies are associated with detailed information. In fact, the localization of the signal in time is made by shifting the wavelet in time and changing the scale causes the localization of the signal in frequency (scale).

Suppose the vector space of signal, $\mathcal{S}$, then if any $f(t) \in \mathcal{S}$ can be defined as $f(t) = \sum_k a_k \phi_k(t)$, the set of function $\phi_k(t)$ can be called an expansion set for the space $\mathcal{S}$. Consequently, the set of the scaling function $\phi_k(t)$ is integer translate of the basic real-valued low-pass scaling function $\phi(t)$. The scaling function can be expressed in terms of a weighted sum of shifted $\phi(2t)$ which is defined as follows [11]:

$$\phi(t) = \sqrt{2} \sum_n h_0(n) \phi_g(2t - n) \tag{2.2}$$

By using (2.2), wavelet can be expressed by a weighted sum of shifted scaling function $\phi(2t)$:

$$\psi(t) = \sqrt{2} \sum_n h_1(n) \phi(2t - n) \tag{2.3}$$

(2.3) gives the prototype or mother wavelet $\psi(t)$ for the classes of expansion function in (2.1).

In (2.2) $h_0(n)$ is low-pass filter and down-sampling operation. Also, in (2.3), $h_1(n)$ is high-pass filter and down-sampling operation. By applying these filters, a useful

parameterization for designing scaling functions and wavelets are provided with desirable properties, such as compact time support and fast frequency decay and orthogonality to low-order polynomials (vanishing moments).

In fact, wavelet $\psi(t)$ and the scaling $\phi(t)$ functions, which are closely associated with each other, are so essential for the multi-resolution formulation as basic functions. The multi-resolution conditions (e.g. good time resolution at high frequencies and good frequency resolution at low frequencies) are satisfied by the majority of useful wavelet systems. In addition, it is important to mention that scaling functions and wavelet functions are two set of functions which are exploited by DWT. These set of basic functions are related to low pass and high pass filters respectively.

Any signal can be generated in terms of wavelet and scaling function [11]:

$$x(t) = \sum_{k=-\infty}^{\infty} c_k \phi(t-k) + \sum_{k=0}^{\infty} \sum_{j=-\infty}^{\infty} d_{j,k} \psi(2^j t - k) \tag{2.4}$$

where c_k is the scaling coefficient and $d_{j,k}$ is the wavelet coefficient. They can be calculated by means of the inner products:

$$c_k = \int_{-\infty}^{\infty} x(t)\phi(t-k)dt \tag{2.5}$$

$$d_{j,k} = 2^{j/2} \int_{-\infty}^{\infty} x(t)\psi(2^j t - k)dt \tag{2.6}$$

A time-frequency analysis of the signal is provided by means of (2.5) and (2.6). That is, we can measure frequency content of the signal at different times where the scale factor *j* and time shift *n* control frequency and time component respectively. Furthermore, we can efficiently compute the coefficients $d_{j,k}$ and c_k from a representation of the signal with desired scale and vice versa based on two octave-

bands, discrete-time Filter Banks (FB) that recursively utilize a discrete-time low-pass filter $h_0(n)$ and high-pass filter $h_1(n)$.

A signal can be easily decomposed into alternative frequency bands by applying high-pass and low-pass filtering to the time domain signal sequentially. First, the input (original) signal $x(n)$ goes through a half band high pass filters $h_1(n)$ and a low pass filter $h_0(n)$. Then, half of the samples of the filtered signal can be omitted because instead of π, the signal, now, has a highest frequency of $\pi/2$ radians. At each level of decomposition, half the number of samples and half the frequency band spanned is produced by filtering and sub-sampling. This procedure is illustrated in Figure 2.1. Finally, by starting to combine all coefficients from the last level of decomposition, the DWT of the original signal is acquired.

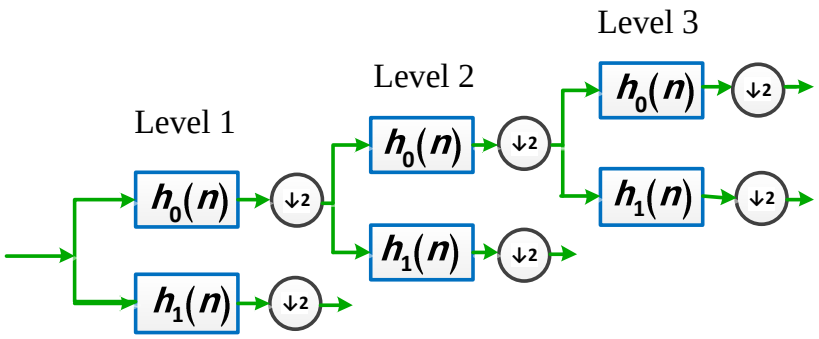

Figure 2.1: The DWT in two-channel FB

Although DWT, which is based on real-valued wavelets, has good properties, there are some fundamental shortcomings: oscillation [11], shift-variance [13, 14], aliasing and lack of directionality. For example, lack of shift invariance, which means that small shifts in the input signal can cause major variations in the distribution of energy between DWT coefficients at different scales. In other words, this results from the down sampling operation at each level. When the input signal is shifted

slightly, the amplitude of the wavelet coefficients varies so much. Shift variance also complicates wavelet-domain processing; algorithms must be made capable of coping with the wide range of possible wavelet coefficient patterns caused by shifted singularities.

2.1.1 Fourier Transform of wavelet and scaling function

Fourier transform of $\phi(t)$ will be required in Chapter 3 and it is defined:

$$\Phi(\omega) = \int_{-\infty}^{\infty} \phi(t) e^{-j\omega t}\, dt \tag{2.7}$$

Moreover, the Discrete-Time Fourier Transform (DTFT) of $h_0(n)$ is expressed:

$$H_0(\omega) = \sum_{n=-\infty}^{\infty} h_0(n) e^{-j\omega n} \tag{2.8}$$

where $i = \sqrt{-1}$ and n is an integer ($n \in \mathbb{Z}$). If $h_0(n)$ is a digital filter such as the Q-shift filter [10], which will be discussed more in detail in Chapter 4, then DTFT of $h_0(n)$ is the frequency response of the filter.

Substituting (2.8) into (2.7) and according to (2.2) results in:

$$\Phi(\omega) = \frac{1}{\sqrt{2}} H_0(\omega/2)\Phi(\omega/2) \tag{2.9}$$

And after iteration of the scaling, it becomes:

$$\Phi(\omega) = \prod_{k=1}^{\infty} \left\{ \frac{1}{\sqrt{2}} H_0\left(\frac{\omega}{2^k}\right) \right\} \Phi(0) \tag{2.10}$$

Fourier transform of $\psi(t)$ is similar to above equations which were applied to scaling function according to (2.3) and after iteration:

$$\Psi(\omega) = H_1\left(\frac{\omega}{2}\right) \left[\prod_{k=2}^{\infty} \frac{1}{\sqrt{2}} H_0(2^{-k}\omega) \right] \Phi(0) \tag{2.11}$$

2.2 Complex Wavelet Transform

We know that Fourier representation is a complex transform with periodic sinusoids in which the imaginary and real parts are constituted by sine and cosine components. These components generate which generate a pair of Hilbert transform. So wavelet and scaling function in $\mathbb{C}$WT are expressed as follows:

$$\psi_c(t) = \psi_r(t) + j\psi_i(t) \tag{2.12}$$

$$\phi_c(t) = \phi_r(t) + j\phi_i(t) \tag{2.13}$$

By considering the Fourier representation, $\psi_r(t)$ is real part and $\psi_i(t)$ is imaginary part of the analytic signal $\psi_c(t)$. If these two parts create a pair of Hilbert transform, then the half of the frequency band supports the analytic signal $\psi_c(t)$. Similar to the Fourier transform, we can also state and analyze any real signal or complex signal by using complex wavelets. The theory of discrete CWTs can be widely classified into two categories. The first one looks for a $\psi_c(t)$ that generates an orthonormal or bi-orthogonal basis [15, 16, 17]. The second one searches for a redundant representation, with both $\psi_r(t)$ and $\psi_i(t)$ separately creating orthonormal or bi-orthogonal bases [18].

All in all, both shift-invariance and good directional selectivity, with only modest increases in signal redundancy and computation load, can be provided by complex wavelet. However, developing a $\mathbb{C}$WT with perfect reconstruction (PR) and ideal filter characteristics has been complicated until recently.

2.3 Dual-Tree Complex Wavelet Transform

The DT-CWT is first proposed by Kingsbury [19]. This is the most successful and useful approach in implementing an analytic wavelet transform. The DT-CWT utilizes two real DWTs such that the real part of the transform is given by the first DWT while the imaginary part is presented by the second DWT. Two different sets of filters are employed by two real wavelet transforms which are used in DT-CWT. These two sets of filters are designed so the overall transform is roughly analytic. Besides, these filters have to meet the PR conditions. In Figure 2.2 the DT-CWT with two sets of filters is illustrated.

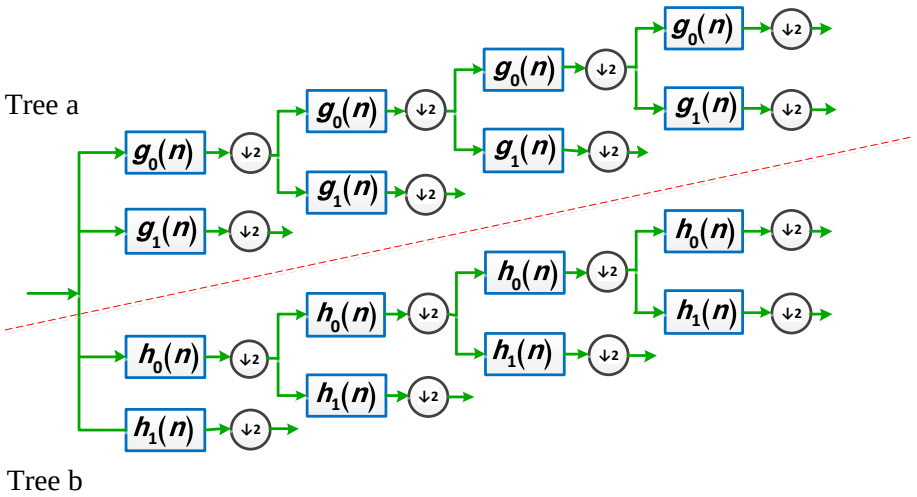

Figure 2.2: Analysis Filter Bank for the DT-CWT [3].

In the upper FB (Tree a), $g_0(n)$ is considered as low-pass filter and $g_1(n)$ is regarded as high-pass filter. Identically, $h_0(n)$ and $h_1(n)$ are considered for the lower FB (Tree b). Both of these trees are real wavelets and denoted by $\psi_g(t)$ and $\psi_h(t)$ for tree a and b respectively. These filters are designed to satisfy PR condition such that the complex wavelet (i.e. $\psi_c(t) = \psi_g(t) + j\psi_h(t)$) is approximately analytic. For

this purpose the filters design such that $\psi_h(t)$ is approximately the Hilbert transform of $\psi_g(t)$ as it is denoted by:

$$\psi_h(t) \approx \mathcal{H}\{\psi_g(t)\} \tag{2.14}$$

According to (2.2) and (2.3) and depending on definition of DT-CWT, it is required to design two low pass filters which are able to satisfy the property in (2.14). For this purpose, one of them must be nearly a half-sample shift of the other so the magnitude and phase functions in frequency domain are expressed as:

$$\left|G_0(e^{j\omega})\right| = \left|H_0(e^{j\omega})\right| \tag{2.15}$$

$$\angle G_0(e^{j\omega}) = \angle H_0(e^{j\omega}) - 0.5\omega \tag{2.16}$$

Because of some reasons [3], (2.15) and (2.16) are approximate for short filters. Thus, several methods have been proposed for filter design for DT-CWT which satisfies some desire property such as: approximately half-sample delay property, PR condition, finite support with FIR filters, vanishing moment and linear phase (for only complex filters). Furthermore, in [13] it was proved that the key to acquiring shift-invariance from the dual-tree structure depends on designing the filter delays at each stage. The Q-shift method [10], which is one of proposed methods for filter design for DT-CWT that we used for analyzing shift-variance will be explain in next section.

2.3.1 The Q-shift filters

It is obvious that we require a group delay for satisfying PR conditions and smoothness feature. Indeed, the Q-shit filters [10] provide a group delay which can be used in wavelet filters in order to generate a combination of properties. For example, the properties such as approximate shift-invariance, good directional selectivity, linear phase, good frequency domain selectivity and so on can be

satisfied by the Q-shift filters. Furthermore, the Q-shift filters minimize the energy of the frequency domain in order to effectively improve the shift-invariance property for DT-CWT. For this purpose, it is crucial that wavelet filters are designed with a group delay of a quarter of sample period.

According to the concept of DT-CWT there exist 2 set of wavelet filters with group delay for 2-band FB (one for tree a and one for tree b). Therefore, one of these group delay filters is $1/4$ of the sample period and another is $3/4$ of the sample period. The latter is the time reverse of the former. In this case, a delay of $1/2$ is produced between tree a and tree b. In [3], the relation between tree a and tree b is stated by:

$$h_0(n) = g_0(N-1-n) \qquad : \qquad 0 \le n \le N-1 \tag{2.17}$$

where N (even) is the length of $g_0(n)$. It must be noticed that the magnitude part of the half-sample delay condition is explicitly satisfied owing to the time-reverse relation between the filters, while the phase part is not precise, (referred to (2.15) and (2.16)).

Accordingly, in order to satisfy the phase condition, we have to design the filters with approximately linear-phase property. Hence, we consider $g_0(n)$ as an approximate linear-phase filter which is expressed as follows [3]:

$$\angle G_0(e^{j\omega}) \approx -0.5(N-1)\omega + 0.25\omega \tag{2.18}$$

That is, it can be said that $g_0(n)$ almost keeps its symmetry property about the $n = 0.5(N-1) - 0.25$ [3]. In other words, there is $1/4$ distance away between this point and the natural one.

Therefore, the Q-shift method generates complex wavelets bases in which the imaginary part (from tree b) is the time reverse of the real part (from tree a).

$$\psi_h(t) = \psi_g(N-1-t) \tag{2.19}$$

Consequently, (2.19) proves that the two significant conditions i.e. PR and linear-phase are completely satisfied by the Q-shift filters at the same time.

We can obtain the filter $G_0(z)\,(\text{length}\,(2N))$ with one quarter delay by considering the filter $G_{L2}(z)\,(\text{length}\,(4N))$ which is defined in half delay and half of the admissible bandwidth. Then we alternatively select the coefficients of $G_{L2}(z)$ in order to acquire $G_0(z)$. If

$$G_{L2}(z) = G_0(z^2) + z^{-1}G_0(z^{-2}) \tag{2.20}$$

where the coefficients of $G_0(z)$ are defined from z^{N-1} to z^{-N} and $G_{L2}(z)$ is linear phase with half sample delay then $G_0(z)$ has one quarter sample delay. Then, we have to specify $G_0(z)$ so that the squared gain of $G_{L2}(z)$ is minimized thus $G_0(z)$ satisfy PR conditions as follows [10]:

$$G_0(z)G_0(z^{-1}) + G_0(-z^{-1})G_0(-z) = 2 \tag{2.21}$$

$$G_0(z) = G_0(z^{-1}) \tag{2.22}$$

Now we can obtain $G_0(z)$ from a poly-phase matrix [20] that express as follows:

$$\begin{bmatrix} G_0(z) \\ z^{-1}G_0(-z^{-1}) \end{bmatrix} = \boldsymbol{\mathcal{R}}(\theta_N)\,\mathbf{Z}\,\boldsymbol{\mathcal{R}}(\theta_{N-1})\,\mathbf{Z}\ldots\boldsymbol{\mathcal{R}}(\theta_1)\begin{bmatrix} 1 \\ z^{-1} \end{bmatrix} \tag{2.23}$$

where $\boldsymbol{\mathcal{R}}(\theta_i) = \begin{bmatrix} \cos\theta_i & \sin\theta_i \\ -\sin\theta_i & \cos\theta_i \end{bmatrix}$ is orthonormal rotation and $\mathbf{Z} = \begin{bmatrix} z & 0 \\ 0 & z^{-1} \end{bmatrix}$ is delay.

According to [18] $G_0(z)$ should have at least one zero at $z=-1$(vanishing moment) thus the angle θ_i in *N* rotations have to sum to $k\pi+\pi/4$. This allows us to optimize $N-1$ angle to obtain $G_0(z)$.To satisfy PR conditions, [20] found the optimal θ_i to minimize the total energy of the frequency response $G_{L2}(z)$ over the range $\pi/3\le\omega\le\pi$. Furthermore, the filter $G_0(z)$ is achieved in terms of $G_{L2}(z)$ which provide some properties such as no aliasing, PR conditions, linear phase and good smoothness.

The coefficients of the Q-shift filter $g_0(n)$ for lengths 8, 12, 18, and 22 are obtained by running the MATLAB codes [21]. And they are shown in Table 2.1. It can be observed that the coefficients of $h_0(n)$ is easily obtained by flipping the $g_0(n)$. In order to satisfy $1/4$ and $3/4$ sample period group delays, $g_1(n)$ and $h_1(n)$ are obtained as well. Finally, according to (2.12), (2.13) and by considering above filters, the complex wavelets and scaling functions can be obtained. In chapter 4 the frequency response of complex wavelet and complex scaling function by using the Q-shift filters of length 8, 12, 18 and 22 are shown in Figures 4.1 and 4.2 respectively.

2.3.2 Dual-Tree Complex Wavelet Transform in Fourier Domain

According to Section 2.2 the Fourier transforms of the wavelets and scaling functions in Tree a and Tree b are given respectively as follows:

$$\Phi_g(\omega)=\frac{1}{\sqrt{2}}\left[\prod_{k=1}^{\infty}G_0(2^{-k}\omega)\right]\Phi_g(0) \tag{2.24}$$

$$\Psi_g(\omega)=G_1(\frac{\omega}{2})\left[\frac{1}{\sqrt{2}}\prod_{k=2}^{\infty}G_0(2^{-k}\omega)\right]\Phi_g(0) \tag{2.25}$$

$$\Phi_h(\omega)=\frac{1}{\sqrt{2}}\left[\prod_{k=1}^{\infty}H_0(2^{-k}\omega)\right]\Phi_h(0) \tag{2.26}$$

$$\Psi_h(\omega) = H_1(\frac{\omega}{2})\left[\frac{1}{\sqrt{2}}\prod_{k=2}^{\infty} H_0(2^{-k}\omega)\right]\Phi_h(0) \qquad (2.27)$$

Then the Fourier transforms of the complex wavelet and scaling function can be obtained accordingly. See (2.12) and (2.13).

Table 2.1: Coefficients of the Q-shift filter $g_0(n)$ for length 8, 12, 18 and 22

8-tap G_0	12-tap G_0	18-tap G_0	22-tap G_0
0.05190908	-0.01522967	0.00142280	-0.00019897
-0.06008402	0.01815856	0.00074129	-0.00013542
-0.05104918	0.02060577	-0.00175206	0.00074080
0.40994913	-0.07884050	-0.00435486	0.00169627
0.53497354	0.00900506	0.02091066	-0.00455923
0.19895626	0.39546502	0.01274698	-0.00798286
-0.03583345	0.54431565	-0.08318752	0.02671233
-0.04882136	0.18423786	0.01584833	0.01008280
	-0.07074785	0.39994096	-0.08866926
	-0.02912820	0.53366076	0.02100178
	0.01205103	0.19704131	0.39978504
	0.01010725	-0.07991466	0.53020029
		-0.03586321	0.20127489
		0.03002088	-0.07917418
		0.00082567	-0.04222550
		-0.00747924	0.03396799
		0.00066137	0.00623307
		-0.00126947	-0.01016548
			0.00024101
			0.00071247
			0.00066580
			-0.00020366

Chapter 3

SHIFT-VARIANCE ANALYSIS

3.1 Introduction

The idea of shift-variance analysis tells if there is a shift in input signal, how the output will treat in terms of this shift. In other words, this kind of analysis measures the difference between the reaction of the system to any shift in input and shifted version of the output. As we know, one of the weaknesses of DWT is shift-variant although this idea is not generally satisfied i.e. in some very special cases; the DWT is characterized as approximate shift-invariance. Accordingly, seeking DWT with good shift-invariance is significant in applications of signal processing e.g. pattern recognition. As a result, numerous researches have been done for this purpose. For better perceiving the meaning of approximate shift-invariance for DWT, we need to understand the idea of μ-shift-invariance which is proposed in [22]. Indeed, μ-shift-invariance defines what it means for some systems (e.g. sampling process) to be shift-invariant.

3.2 The Sampling Process

3.2.1 The Mathematical Description

We consider two complex signals x, ψ in continuous-time domain. Then, the inner product of them in a Hilbert space L^2 is defined as follows:

$$\langle x, \psi \rangle = \int_{\mathbb{R}} \psi^*(t) x(t) dt \quad , \quad x, \psi \in L^2 \tag{3.1}$$

Suppose a scalar $T > 0$, a sequence of signal ψ is defined as:

$$\psi_n(\cdot) = \psi(\cdot - nT),\ n \in \mathbb{Z} \tag{3.2}$$

A linear system $\mathcal{S}$, which could characterize a generalized uniform sampling process [8] where ψ and T state the kernel and period of sampling respectively, can be defined via the inner product as follows:

$$\mathcal{S}(L^2 \to \ell^2) : x \mapsto y \quad \text{and in Fourier domain} \qquad \mathcal{S} : \hat{x} \mapsto \hat{y} \tag{3.3}$$

Regarding to (3.1) and (3.2) inner product of x and the sequence of signal ψ defines the discrete-time of output in the Hilbert space ℓ^2:

$$y = \{y_n\}_{n \in \mathbb{Z}} \qquad \text{with} \qquad y_n = \langle x, \psi_n \rangle \tag{3.4}$$

It must be noticed that the input and output of $\mathcal{S}$ are continuous-time and discrete-time respectively. System $\mathcal{S}$ can be described as in Figure 3.1 where the $h(t)$ is the filter and also the input-output relation of $\mathcal{S}$ is described in the time-domain and Fourier domain respectively as follows:

$$\mathcal{S} : y_n = \int_{\mathbb{R}} h(nT - t)x(t)dt \tag{3.5}$$

$$\mathcal{S} : Y(e^{jT\omega}) = \frac{1}{T} \sum_{K \in \mathbb{Z}} H(\omega - 2k\pi/T)X(\omega - 2k\pi/T) \tag{3.6}$$

(3.6) can be considered as sampling process and simplified as:

$$\mathcal{S} : Y(e^{jT\omega}) = \frac{1}{T} \mathbf{H}(\omega/T)X(\omega/T) \tag{3.7}$$

where the sampling vector of H is defined by:

$$\mathbf{H}(\omega) = \{H(\omega - 2k\pi/T)\}_{K \in \mathbb{Z}} \tag{3.8}$$

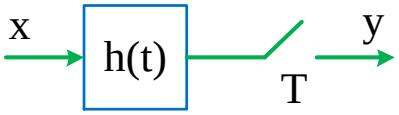

Figure 3.1: The generalized sampling process $S(h(t) = \psi^*(-t))$.

3.2.2 System-Norm

In (3.3), we defined a linear system $\mathcal{S}$, now we can express the system norm for this system by:

$$\|\mathcal{S}\| = \sup\{\frac{\|\mathcal{S}x\|_{l^2}}{\|x\|_{L^2}} : x \neq 0\} \tag{3.9}$$

where sup indicates the supremum. Note that, we can characterize the least upper bound by using the induced-norm in which the system can magnify the input signal *x*. It is assumed that $\|\mathcal{S}\| < \infty$.

According to Figure 3.1 and the general definition of sampling process $\mathcal{S}$ [8], (3.10) defines the induced-norm of the system as:

$$\|\mathcal{S}\| = \frac{1}{\sqrt{T}}\|\mathbf{H}\|_{\infty} \tag{3.10}$$

where the ∞-norm $\|\mathbf{H}\|_{\infty}$ is defined by $\sup\{\|\mathbf{H}(\omega)\| : \omega \in [0, 2\pi/T)\}$ with

$$\|\mathbf{H}(\omega)\| = (\sum_{K\in\mathbb{Z}} |H(\omega - 2k\pi/T)|^2)^{1/2} \tag{3.11}$$

3.3 The μ-Shift-Invariance System

We can consider any system as shift-invariant if a shift occurs in input, then a shift also happens in output. Absolutely, this system is exactly shift-invariant when the shift's amount of output is identical to that of the input. For the aim of sampling processing (Section 3.2), because the input and output are defined as continuous-time and discrete-time domains respectively, it is intensively required to clarify the

meaning of shift-invariance. Considering the sampling process $\mathcal{S}$ in Section 3.2, when the input is shifted by $\tau \in \mathbb{R}$, it is expected that the τ/T shift must happen in output.

The discrete-time system is called a discrete-time shift operator in $\mathcal{B}$ [8] if:

$$\mathcal{D}_{\mathcal{B}}^{\alpha} : Y(e^{j\omega}) \mapsto e^{-j\alpha\omega} Y(e^{j\omega}), \quad \omega \in \mathcal{B}, \alpha \in \mathbb{R}, \mathcal{B} \in \mathbb{B} \tag{3.12}$$

where α and $\mathcal{B}$ are called the amount of the shift and the admissible band respectively. Furthermore, $\mathbb{B}$ is the set of all admissible bands and $\mathcal{D}_{\mathcal{B}}^{\alpha}$ is the discrete-time shift operator that is linear and shift-invariant. Therefore, the discrete-time shift operator becomes fractional and it depends on the choice of $\mathcal{B}$ [22] if α is not an integer.

A system is called to be μ-Shift-invariance with factor α (i.e. it is unique for μ-shift-invariance $\mathcal{S} \neq 0$) and in $\mathcal{B}$ if for any input x the react to $x(\cdot - \tau)$ is determined by [8]:

$$\mathcal{D}_{\mathcal{B}}^{\alpha\tau} \mathcal{S}x \quad \text{i.e.} \quad e^{-j\alpha\tau\omega} Y(e^{j\omega}), \quad \omega \in \mathcal{B}, \alpha \in \mathbb{R}, \tau \in \mathbb{R} \tag{3.13}$$

where $\alpha = 1/T$ is defined for the sampling process. In addition to the definition of discrete-time shift operator which was stated in (3.12), continuous-time shift operator is denoted by:

$$\mathcal{D}^{\tau}(L^2 \to L^2) : x(\cdot) \mapsto x(\cdot - \tau) \tag{3.14}$$

Then, the error system is expressed as follow:

$$\mathcal{K}_{\tau,\mathcal{B}} = \mathcal{S}\mathcal{D}^{\tau} - \mathcal{D}_{\mathcal{B}}^{\alpha\tau}\mathcal{S} \tag{3.15}$$

where $\mathcal{K}_{\tau,\mathcal{B}}$ is the error system. This error is also referred to the commutator. Note that, when $\mathcal{K}_{\tau,\mathcal{B}} = 0$, the system $\mathcal{S}$ is μ-shift-invariant.

3.4 Shift-Variance Analysis

3.4.1 Shift-Variance Level and Shift-Variance Measure

Shift-variance can be characterized by presenting: a) the Shift-Variance Level (SVL) and b) the Shift-Variance Measure (SVM) that these two quantities always exist and are unique. In fact, The SVL describes the amount of distance between the system and the set of systems which are so called μ-shift-invariant. Also, the SVM is equal to the SVL divided by two times of the system norm.

According to (3.15), the generalized commutator of linear system specifies amount of the SVL and SVM. Let $\mathcal{S}: L^2 \to l^2$ in terms of shift τ and in band $\mathcal{B}$, the SVL is defined by [8]:

$$\mathcal{K}(\mathcal{S}) = \inf_{\mathcal{B}\in\mathbb{B}} \{\sup_{\tau\in\mathbb{R}} \left\| \mathcal{K}_{\tau,\mathcal{B}} \right\|\} \tag{3.16}$$

Then, SVL is defined by:

$$\nu(\mathcal{S}) = \frac{\mathcal{K}(\mathcal{S})}{2\|\mathcal{S}\|} \qquad \mathcal{S} \neq 0 \text{ [1]} \tag{3.17}$$

In [8], it was proved that:

$$0 \le \nu(\mathcal{S}) \le 1 \tag{3.18}$$

According to above equation, we can say that when $\nu(\mathcal{S}) = 1$, system $\mathcal{S}$ is completely shift-variant and also when $\nu(\mathcal{S}) = 0$, system $\mathcal{S}$ is μ-shift-invariant.

3.4.2 Analytical Formula for SVL and SVM

By considering the sampling vector in (3.8) which is described in Section 3.2.1 and for the sampling process $\mathcal{S}$ in Figure 3.1, the formulas for analysis the SVL and SVM can be obtained.

[1] In the case of $\mathcal{S} = 0$, since $\mathcal{K}(\mathcal{S}) = 0$, we define $\nu(\mathcal{S}) = 0$

The continuous-time shift operator and the discrete-time shift operator are defined respectively by:

$$\mathcal{SD}^{\tau} : X(\omega) \mapsto \frac{1}{T} e^{-j\omega\tau/T} \mathbf{H}^{T}(\omega/T) \mathbf{W}_{\tau} X(\omega/T), \qquad \mathbf{W}_{\tau} = \operatorname{diag}[e^{j2k\pi/T}]_{k\in\mathbb{Z}} \quad (3.19)$$

$$\mathcal{D}_{\mathcal{B}}^{\tau/T}\mathcal{S} : X(\omega) \mapsto \frac{1}{T} e^{-j\omega\tau/T} \mathbf{H}^{T}(\omega/T) X(\omega/T), \quad \omega \in \mathcal{B} \quad (3.20)$$

By applying (3.16) and (3.17) and considering the continuous-time shift operator and the discrete-time shift operator which were defined in (3.19) and (3.20), the SVL of sampling process $\mathcal{S}$ with respect to τ and in $\mathcal{B}$ is expressed as follows:

$$\mathcal{K}(\mathcal{S}) = \inf_{\mathcal{B}\in\mathbb{B}} \{ \sup_{\tau\in(0,T/2]} \{ \frac{2}{\sqrt{T}} \left\| \mathbf{\Sigma}_{\tau} \mathbf{H} \right\|_{\infty} \} \qquad : \qquad \left\| \mathcal{K}_{\tau,\mathcal{B}} \right\| = \frac{2}{\sqrt{T}} \left\| \mathbf{\Sigma}_{\tau} \mathbf{H} \right\|_{\infty} \quad (3.21)$$

And therefore we can express the SVM as:

$$\nu(S) = \frac{\inf_{\mathcal{B}\in\mathbb{B}} \{ \sup_{\tau\in(0,T/2]} \{ \frac{2}{\sqrt{T}} \left\| \mathbf{\Sigma}_{\tau} \mathbf{H} \right\|_{\infty} \}}{\left\| \mathbf{H} \right\|_{\infty}} \quad (3.22)$$

Particularly, for better perceiving the equation in (3.21), we can express it precisely as follows [8]:

$$\mathcal{K}(\mathcal{S}) = \inf_{\omega_0\in\mathbb{R}} \left\{ \sup_{\tau\in(0,T/2]} \left\{ \sup_{\omega\in[\omega_0,\omega_0+2\pi)} \left\{ 2 \left[\sum_{k\in\mathbb{Z}} (\sin^2 k\pi\tau) |H^2(\omega - 2k\pi)| \right]^{1/2} \right\} \right\} \right\} \quad (3.23)$$

where the filter *H* (in the Fourier domain) is computed in defining band. It must be noticed that just ω_0 has effect on parameterizing this band and also we may acquire the optimal value across the subset of defining band:

$$\{[\omega_0, \omega_0 + 2\pi)\}_{\omega_0\in\mathbb{R}} \quad (3.24)$$

In particular, for either $\omega_0 \in \mathbb{R}$, two successive one-dimensional optimizations are employed to find the two nested suprema. Then, the determination is finalized by

searching for ω_0. All above mentioned issues will be applied for analyzing the shift-variance of real DWT in the next section.

3.5 Shift-Variance Analysis of Wavelet transform

Generally, we can say that DWT cannot satisfy the shift-invariant property [2] although some DWTs are approximately shift-invariant [3]. In this section, by applying what was mentioned in the preceding chapter, the analysis of shift-variance properties will be done [8].

Consider $\psi(t)$ as an admissible wavelet function in L^2 in (2.1), according to definition of the DWT for each j a sampling process is defined as:

$$\mathcal{S}_j : x(t) \mapsto \left\{ \left\langle x(t), \psi_{j,k}(t) \right\rangle \right\}_{k \in \mathbb{Z}} \tag{3.25}$$

Then by regarding to linear system in Figure 3.1, the filter $h(t)$ is stated by:

$$h(t) = \psi^*_{j,0}(-t) \tag{3.26}$$

And in the Fourier transform is expressed as follows:

$$H(\omega) = \Psi^*_j(\omega) = 2^{j/2} \Psi^*(2^j \omega) \tag{3.27}$$

Consequently, the norm and the SVL of sampling process $\mathcal{S}_j$ in DWT are obtained respectively by:

$$\left\| \mathcal{S}_j \right\| = \sup_{\omega \in [0, 2\pi/T)} \left\| \mathbf{\Psi}_j \right\| = \left\| \mathbf{\Psi}_j \right\|_\infty = 2^{j/2} \left\| \mathbf{\Psi} \right\|_\infty \tag{3.28}$$

$$\mathcal{K}(\mathcal{S}_j) = \inf_{\mathcal{B} \in \mathbb{B}} \{ \sup_{\tau \in (0, T/2]} \{ 2 \, [2^{j/2} \left\| \mathbf{\Sigma}_\tau \mathbf{\Psi} \right\|_\infty] \} \tag{3.29}$$

In the above equations, it can be observed that there is a relation between two values of the SVL at scale j and scale $j = 0$ as:

$$\mathcal{K}(\mathcal{S}_j) = 2^{j/2} \mathcal{K}(\mathcal{S}_0) \tag{3.30}$$

So, according to (3.28) and (3.30) the SVM in DWT is equal for all scale j i.e. $\nu(\mathcal{S}_j) = \nu(\mathcal{S}_0)$. Accordingly, the SVL and SVM can be computed in the zeroth scale (i.e., the SVL and SVM of $\mathcal{S}_0$).

Chapter 4

ANALYSIS RESULTS

4.1 Introduction

For better understanding those were mentioned in previous chapters, the analysis of shift-variance on the DT-CWT and the scaling function will be done in this chapter. In fact, the SVL and SVM of the DT-CWT and the scaling function will be examined each with the Q-shift filters of length 8, 12, 18, and 22.

4.2 Analysis Results

In order to analyze shift-variance, we plot the magnitude spectra of the dual-tree complex wavelets $\|\Psi_c(\omega)\|$ in Figure 4.1; the magnitudes of the modulated vector $\|\boldsymbol{\Psi}_c(\omega)\|$ are also given in Figure 4.1. The magnitude spectra of the complex scaling function $\|\Phi_c(\omega)\|$, and the magnitude of modulated vector $\|\boldsymbol{\Phi}_c(\omega)\|$ is illustrated in Figure 4.2. These illustrations for both DT-CWT and the scaling function are performed for each the Q-shift filter of length 8, 12, 18, and 22 respectively.

It is important to mention that we can approximate both the modulated vectors $\|\boldsymbol{\Psi}_c(\omega)\|$ and $\|\boldsymbol{\Phi}_c(\omega)\|$ if we take eleven sampling (i.e. $-5 \le k \le 5$). Thus, we can obtain the norm $\|\mathcal{S}\|_\infty$ for DT-CWT and the scaling function by regarding to the maximum value of the magnitude spectra of modulated vector $\|\boldsymbol{\Psi}_c(\omega)\|$ and $\|\boldsymbol{\Phi}_c(\omega)\|$ respectively.

Moreover, some indication related to defining band $\mathcal{B}$ is provided in Figure 4.1 and 4.2 where depict the DT-CWT's magnitude spectra specifically $\mathcal{B} = (\omega_0, \omega_0 + \pi)$ with $\omega_0 \approx 0.5$ and the scaling function's magnitude spectra with $\omega_0 \approx -1.5$. In general, it would be very challenging to theoretically obtain the optimality of defining band. However, the optimal defining band can be acquired by regarding the level set. This issue is completely discussed in more detail in [8]. In Table 4.1 and Table 4.2, the system norm and the defining band of each length of the Q-shift filters are tabulated for DT-CWT and for the scaling function respectively.

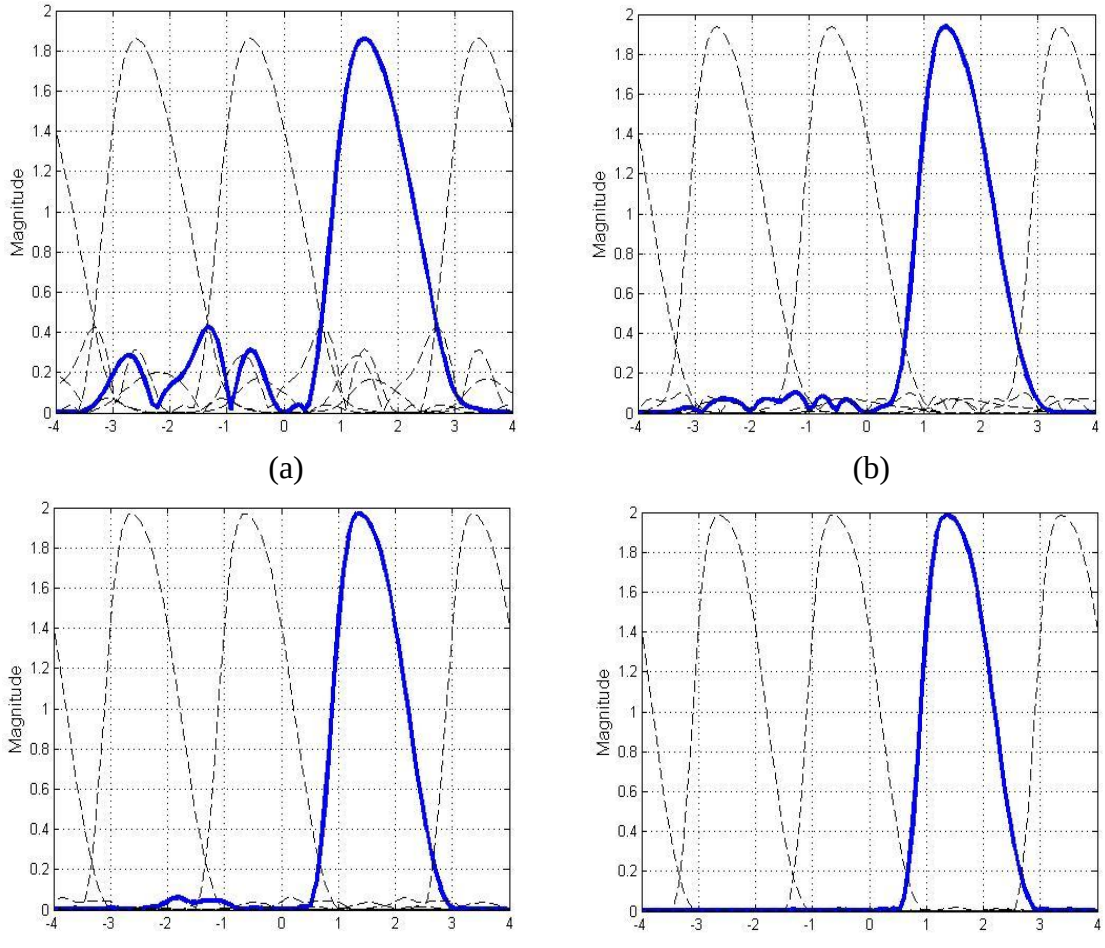

Figure 4.1: Magnitude spectra $\|\Psi_c(\omega)\|$ (solid line) and $\|\boldsymbol{\Psi}_c(\omega)\|$ (dashed line) of the complex wavelets using Q-shift filters: (a) length 8, (b) length 12, (c) length 18, and (d) length 22.

It can be observed that the stop-band attenuation is improved when the length of Q-shift filters increases. This improvement is explicitly illustrated in Figure 4.1 for DT-CWT and Figure 4.2 for the scaling function. In other words, the stop-band is attenuated in the Q-shift filter of length 8 less than in the Q-shift filter of length 22. If the length increases, the stop-band will be attenuated more and more. Furthermore, by increasing the length of the Q-shift filters, smoothness and shift-invariant properties are improved more and more for the DT-CWT and the scaling function in defining band. This improvement in smoothness and shift-invariance, which are very important properties in DT-CWT, can be detected in Figure 4.1 for the complex wavelets and in Figure 4.2 for the complex scaling function as well.

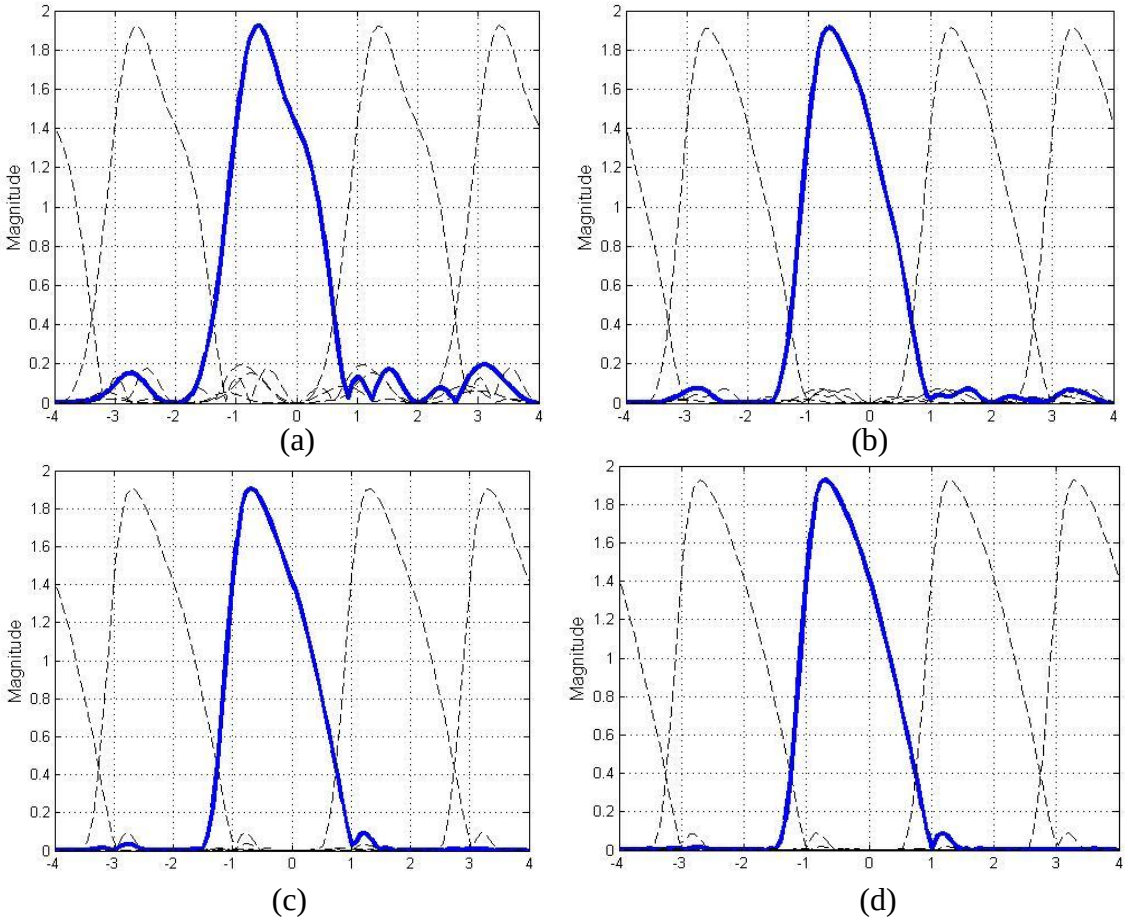

Figure 4.2: Magnitude spectra $\|\Phi_c(\omega)\|$ (solid line) and $\|\boldsymbol{\Phi}_c(\omega)\|$ (dashed line) of the complex scaling functions using Q-shift filters: (a) length 8, (b) length 12, (c) length 18, and (d) length 22.

As it was explained, the SVL $\left\|\mathcal{K}_{\tau,\mathcal{B}}\right\|$ is a function of two variables: the amount of shift τ and the starting frequency ω_0 in the admissible band. Hence, the changes in the value of the SVL is affected by two variables τ and ω_0. The SVL is graphically depicted in Figure 4.3 and 4.4 for the dual-tree complex wavelets and the complex scaling function using the Q-shift filters of length 8, 12, 18, and 22 respectively. The effect of two variables ω_0 and τ on the SVL can be perceived in the figures. Note that these figures are shown in band [-2π, 3π] for better visualizing the distinction of the admissible band.

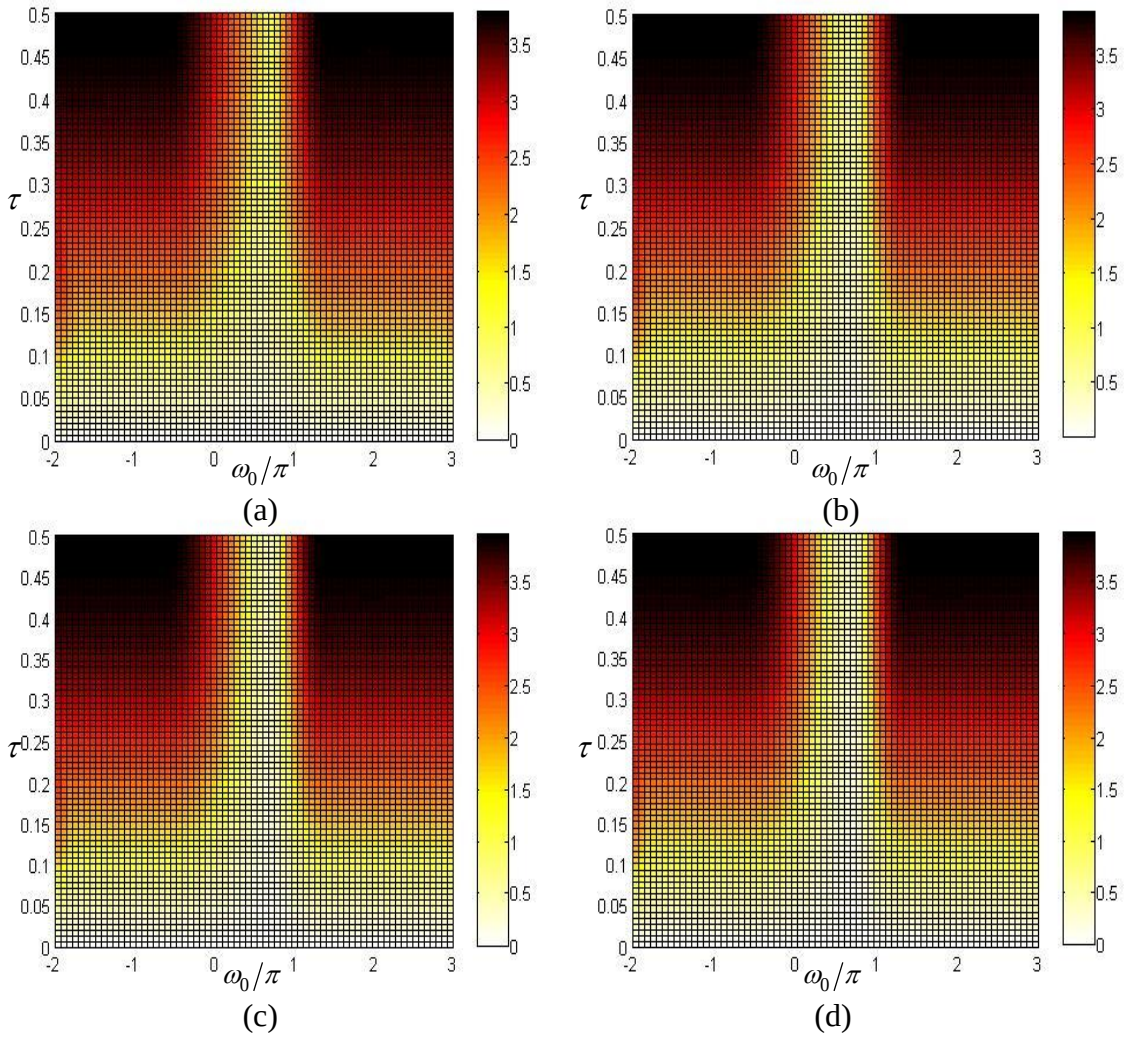

Figure 4.3: The shift-variance level of the Dual-tree complex wavelets using Q-shift filters: (a) length 8, (b) length 12, (c) length 18, and (d) length 22.

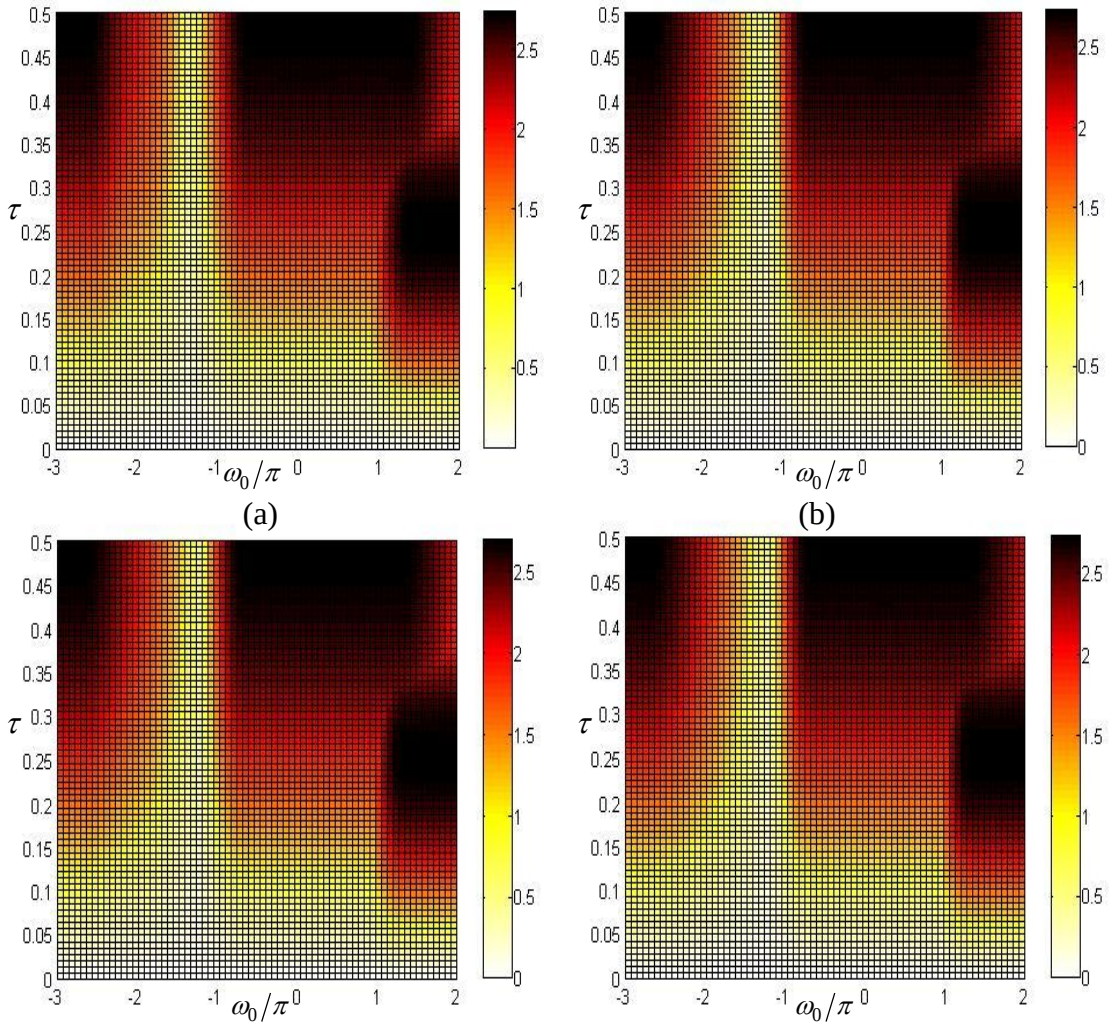

Figure 4.4: The shift-variance level of the complex scaling functions using Q-shift filters: (a) length 8, (b) length 12, (c) length 18, and (d) length 22.

By considering all of graphical figures (DT-CWT and the scaling function), it can be seen that when τ is less than 0.05, the values of SVL are very small. This is always true irrespective of the starting frequency ω_0 and the defining band. For fixed $\mathcal{B}$, by increasing τ, the SVL is also increased although it must be noticed that this is not always the case. Therefore, the values of the SVL stabilize small for any value of shift τ if the defining band is properly specified. In addition, complex DWTs satisfy the property of near shift-invariance. As we know, the DT-CWT and the scaling function are also considered as the complex DWT thus near shift-invariance property

can be also explained in them. In addition, Table 4.1 and Table 4.2 are used for tabulating the numerical results of the shift-variance analysis for both DT-CWT and the scaling function, and defining bands are also presented in these tables respectively.

By considering Table 4.1, we see that the DT-CWT with the Q-shift filters has good shift-invariance measure, i.e. $0 < v(\mathcal{S}) < 0.5$. Indeed, the SVM is reduced by increasing the length of the filters. For example, the Q-shift filter of length 8 is less shift-invariance than the Q-shift filter of length 22.

Table 4.1: shift-variance analysis of DT-CWT using the Q-shift filters of different lengths

DT-CWT	Norm $\|\mathcal{S}\|$	Band $\mathcal{B}$	Shift-variance level $\mathcal{K}(\mathcal{S})$	Shift-variance measure $v(\mathcal{S})$ (%)
Q-shift 8	1.9196	[0.6904π, 2.6904π)	1.1731	30.56
Q-shift 12	1.9407	[0.6653π, 2.6653π)	0.6784	17.47
Q-shift 18	1.9702	[0.6685π, 2.6685π)	0.4905	12.45
Q-shift 22	1.9854	[0.6676π, 2.6676π)	0.3436	8.65

Table 4.2: shift-variance analysis of the scaling function using the Q-shift filters of different lengths

Scaling function	Norm $\|\mathcal{S}\|$	Band $\mathcal{B}$	Shift-variance level $\mathcal{K}(\mathcal{S})$	Shift-variance measure $v(\mathcal{S})$ (%)
Q-shift 8	1.9200	[-1.3768π, 0.6232π)	0.8933	23.26
Q-shift 12	1.9088	[-1.3034π, 0.6966π)	0.8363	21.90
Q-shift 18	1.8758	[-1.2562π, 0.7438π)	0.8932	23.81
Q-shift 22	1.8897	[-1.2466π, 0.7534π)	0.7958	21.06

According to Figure 3.1, we consider DT-CWT and the scaling function as two systems in order to illustrate shift-invariance property in both of them. For this purpose we compare the outputs of an input signal $x(t)$ and its shifted version. This input signal is a simple pulse signal in continuous-time and we shift it by ten units in time (Figure 4.5). We can obtain the outputs by considering equation (3.5) (i.e. $x(t)$ is an input as well as the DT-CWT and the scaling function are sampling kernels). The input signal and the outputs corresponding on the DT-CWT and the scaling function for the Q-shift filters of lengths 8 and 22 are shown in Figures 4.6-4.9 respectively. These figures illustrate that the shift-invariance property is mostly improved for Q-shift filter of length 22.

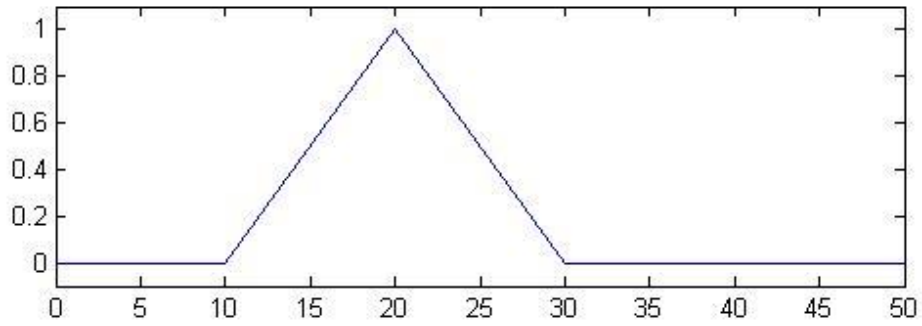

(a)

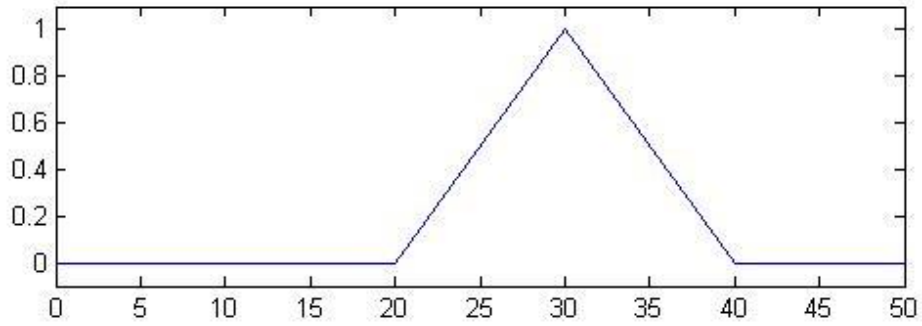

(b)

Figure 4.5: (a) The input signal $x(t)$ and (b) the shifted version of input signal $x(t+10)$

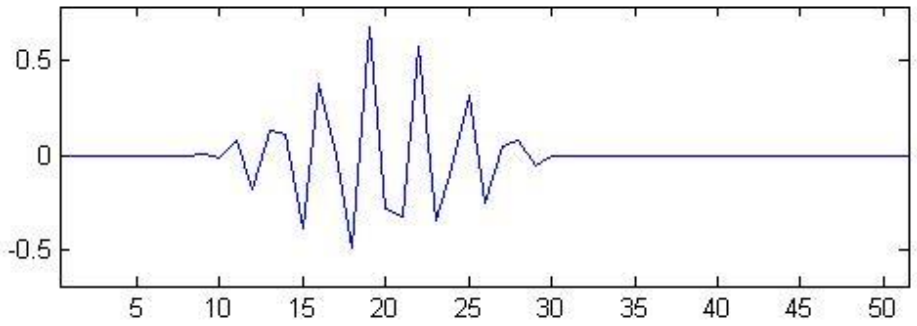

(a)

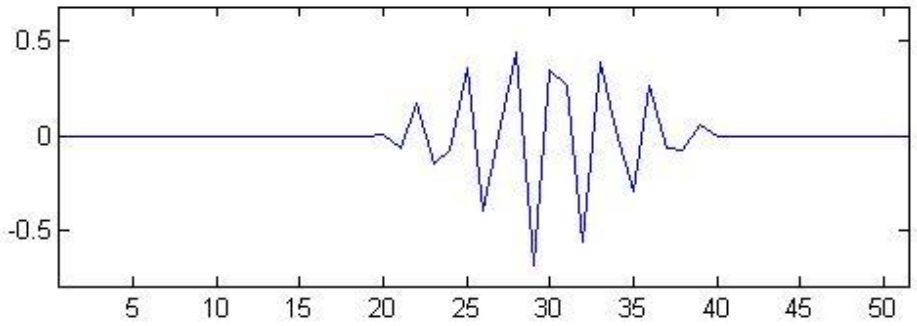

(b)

Figure 4.6: The real part of the output of DT-CWT using Q-shift of length 8 in terms of the input (a) and the shifted version of input (b).

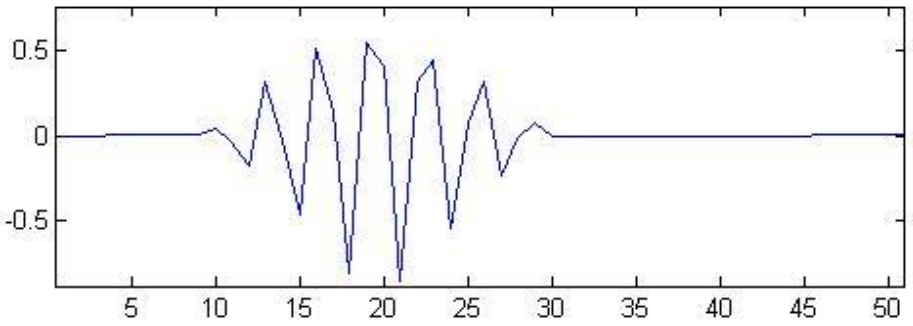

(a)

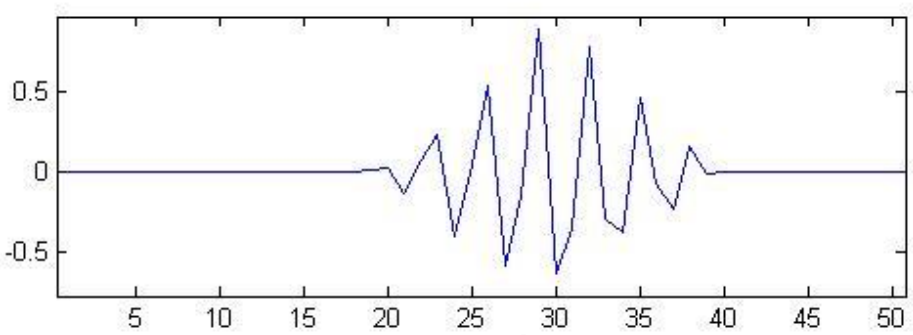

(b)

Figure 4.7: The real part of the output of the complex scaling function using Q-shift of length 8 in terms of the input (a) and the shifted version of input (b).

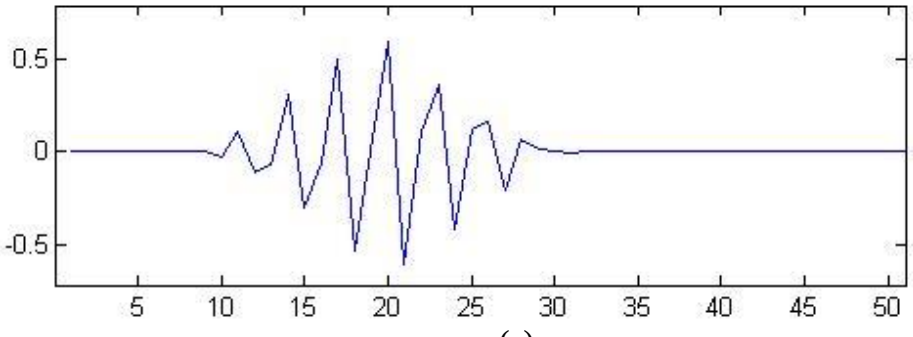

(a)

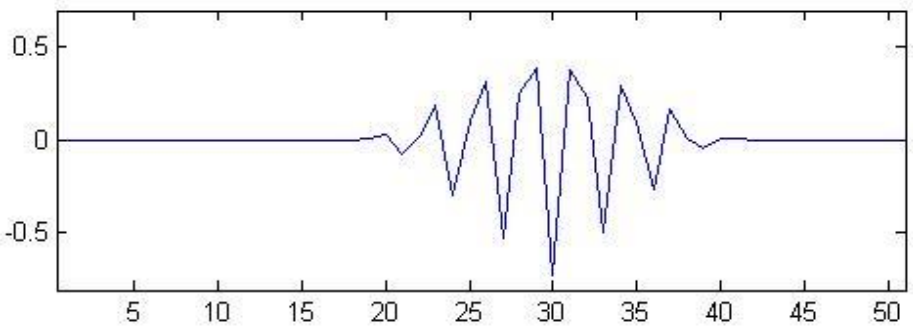

(b)

Figure 4.8: Real part of the output of DT-CWT using Q-shift of length 22 in terms of the input (a) and the shifted version of input (b).

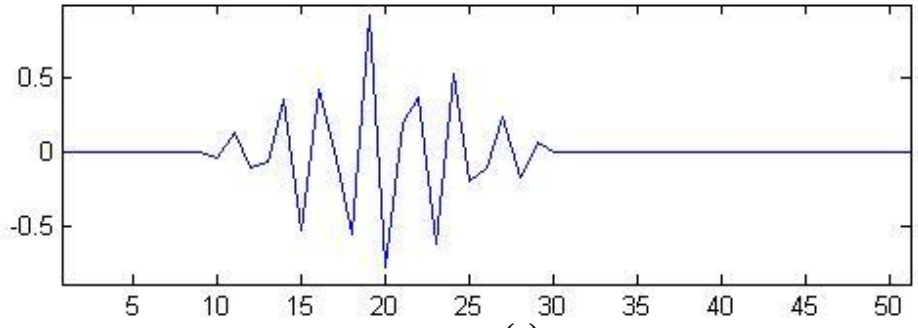

(a)

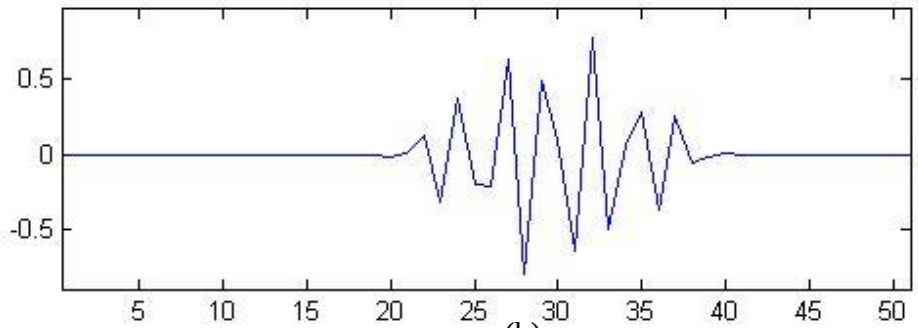

(b)

Figure 4.9: The output of the complex scaling function using Q-shift of length 22 in terms of the input (a) and the shifted version of input (b). (real (blue), imaginary (black))

In Figure 4.10 and 4.11, the results of the SVM of the DT-CWT and the complex scaling function are compared with the results of the SVM of the single-tree complex wavelet and real scaling function with the Q-shift filters of length 8, 12, 18, and 22. In Figure 4.10, the SVM of DT-CWT and the single-tree wavelet for Q-shift filters of length 8, 12, 18, and 22 are provided with each other for better comparison. Generally speaking, the SVM of the DT-CWT is fallen gradually by increasing filter's length. In the other words, the Q-shift filters of long length tend to have less SVM, and the SVM reaches the lowest point in the 22-length Q-shift filters, i.e., it has the best shift-invariance measure in this case (among all the Q-shift filter considered). We check the lengths of Q-shift for more tap (e.g. 24 and 26); and not much improvement is observed. In addition the SVM of the single-tree wavelet are nearly steady in the Q-shift filters of different lengths.

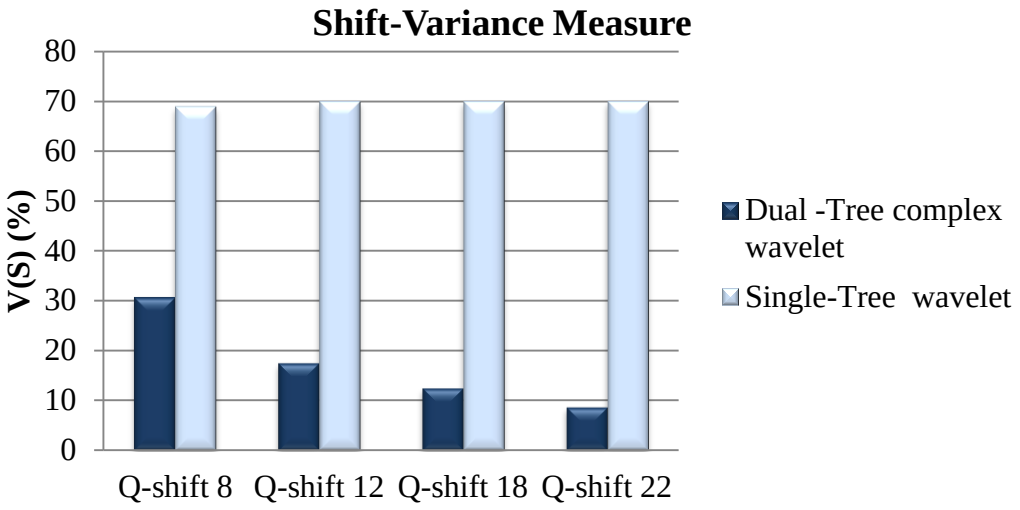

Figure 4.10: The shift-variance measure of the dual-tree complex wavelets and the single-tree wavelet in Q-shift filters of length 8, 12, 18 and 22.

In Figure 4.11, the SVM of the complex scaling function is compared with ones of real scaling function. Generally speaking the SVM of both are nearly steady in Q-shift filter of different lengths but the values of SVM of complex scaling function is very smaller than the values of SVM of real scaling function with same length of Q-shift filter.

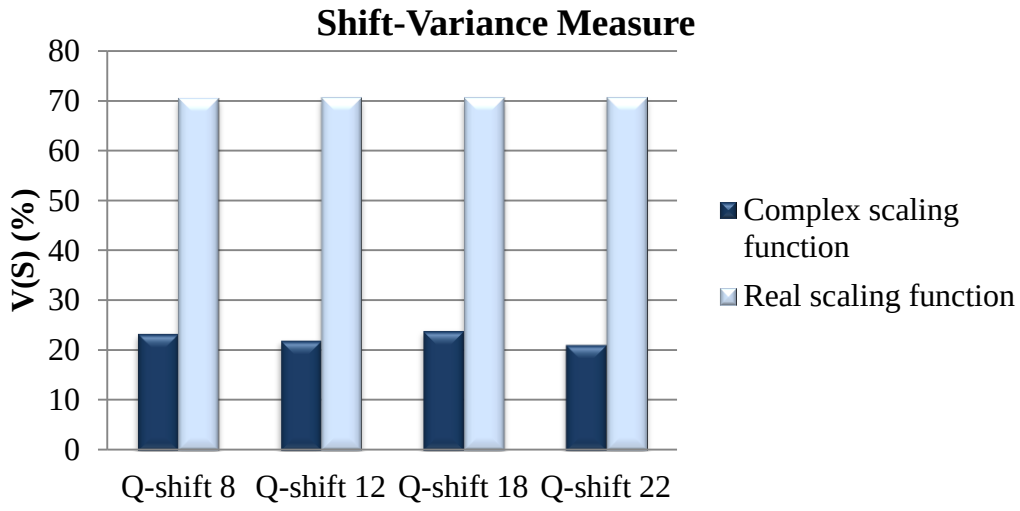

Figure 4.11: The shift-variance measure of the complex scaling function and real scaling function in Q-shift filters of length 8, 12, 18 and 22.

Chapter 5

CONCLUSION

5.1 Conclusion

In this thesis, the shift-variance analysis was applied to dual-tree complex wavelet transforms (DT-CWT) and the scaling functions. In particular, we studied the DT-CWT and the scaling function with Q-shift filter implementation.

We used Kingsbury's approach to obtain the coefficients of Q-shift filters. These coefficients were designed in order to provide approximately shift-invariance DT-CWT with a quarter sample period group delay.

To study shift-variance in DT-CWT and the scaling function analytically, we considered a linear system with continuous-time and discrete-time in input and output respectively. For this aim, the sampling process in frequency domain was adopted, and we obtained the output as an inner product between input and the sampling kernel. Then, the system norm can be computed for both the DT-CWT and the scaling function.

Furthermore, we analyzed shift-variance for the DT-CWT and the scaling function as systems, which are not μ-shift-invariance, by obtaining the quantitative measures: the shift-variance level (SVL) and the shift-variance measure (SVM). The results in this thesis show the shift-variance analysis of DT-CWT and the scaling function with

Q-shift filters of length 8, 12, 18, and 22. We obtained the values of system norm, SVL and SVM in admissible band for DT-CWT and the scaling function with Q-shift filters of different lengths.

We observed that when the length of Q-shift filters increases the value of the SVM of the DT-CWT decreases. This means that the shift-invariance property of DT-CWT was improved by increasing the length of Q-shift filters. Moreover, the shift-invariance property of the scaling function was nearly steady in the Q-shift filters of different lengths.

5.2 Future work

Based on the shift-variance analysis in DT-CWT and the scaling function, we can improve the shift-invariance property of them by designing new filters. In addition it may be possible to analyze shift-variance of other transforms and to compare them.

REFERENCES

[1] J. C. Pesquet, H. Krim, and H. Carfantan, "On time invariance of wavelet decompositions," *IEEE Trans. Signal Process*., vol. 44, pp. 1964–1970, Aug. 1996.

[2] N. G. Kingsbury, "Complex wavelets for shift-invariant analysis and filtering of signals," *Appl. Comput. Harmon. Anal.,* vol. 10, no 3, pp. 234–253, May 2001.

[3] I. W. Selesnick, R. G. Baraniuk, and N. G. Kingsbury, "The dual-tree complex wavelet transform," *IEEE Signal Process. Mag.*, vol. 22, no 6, pp. 123–151, Nov. 2005.

[4] F. C. A. Fernandes, R. L. C. van Spaendonck, and C. S. Burrus, "A new framework for complex wavelet transforms," *IEEE Trans. Signal Process.*, vol. 51, pp. 1825–1837, Jul. 2003.

[5] T. Matsuo, Y. Yoshida, and N. Nakamori, "Proposal of shift insensitive wavelet decomposition for stable analysis," *IEICE Trans. Fundam.*, vol. E88-A, pp. 2087–2099, Aug. 2005.

[6] E. P. Simoncelli, W. T. Freeman, E. H. Adelson, and D. J. Heeger, "Shiftable multi-scale transforms," *IEEE Trans. Inform. Theory*, vol. 38, pp. 587–607, Mar. 1992.

[7] T. Aach, and H Führ, "Shift Variance Measures for Multirate LPSV Filter Banks With Random Input Signals," *IEEE Trans. Signal Process.*, vol. 60, no. 10, pp. 5125-5134, Oct. 2012.

[8] R. Yu, "Shift-variance Analysis of Generalized Sampling Processes," *IEEE Trans. Signal Process.*, vol. 60, pp. 2840–2850, Mar. 2012.

[9] R. Yu, "Shift-Variance Measure of Multichannel Multirate Systems," *IEEE Trans. Signal Process.*, vol. 59, pp. 6245–6250, Dec. 2011.

[10] N. G. Kingsbury, "Design of q-shift complex wavelets for image processing using frequency domain energy minimization", in *Proc. of IEEE Int. Conf. Image Processing, Barcelona* , vol. 1, pp. 1013 - 1016, Sep. 2003.

[11] C. S Burrus, R.A Gopinath and H. Guo, "*Introduction to Wavelets and Wavelet Transforms*," Prentice Hall, New Jersey, 1998.

[12] H. Choi, J. Romberg, R.G. Baraniuk, and N. Kingsbury, "Hidden Markov tree modeling of complex wavelet transforms," in *Proc. IEEE Int. Conf. Acoust., Speech, Signal Processing (ICASSP)*, Jun 5–9, 2000, vol. 1, pp. 133–136.

[13] N. G. Kingsbury, "Image processing with complex wavelets," *Philos. Trans. R. Soc. London A, Math. Phys. Sci.*, vol. 357, no. 1760, pp. 2543–2560, Sept. 1999.

[14] P. L. Dragotti and M. Vetterli, "Wavelet footprints: Theory, algorithms, and appli cations," *IEEE Trans. Signal Processing,* vol. 51, no. 5, pp. 1306–1323, May 2003.

[15] H. F. Ates and M. T. Orchard, "A nonlinear image representation in wavelet domain using complex signals with single quadrant spectrum," in *Proc. Asilomar Conf. Signals, Systems, Computers,* 2003, vol. 2, pp. 1966–1970.

[16] B. Belzer, J. M. Lina, and J. Villasenor, "Complex, linear-phase filters for efficient image coding," *IEEE Trans. Signal Processing,* vol. 43, no. 10, pp. 2425–2427, Oct. 1995.

[17] J. M. Lina and M. Mayrand, "Complex Daubechies wavelets," *Appl. Comput. Harmon. Anal.*, vol. 2, no. 3, pp. 219–229, 1995.

[18] I. Daubechies, "The wavelet transform, time-frequency localization and signal analysis," *IEEE Trans. Inform. Theory,* vol. 36, no. 5, pp. 961–1005, Sept. 1990.

[19] N. G. Kingsbury, "The dual -tree complex wavelet transform: A new technique for shift invariance and directional filters," in *Proceeding of the* 8^{th} *IEEE DSP Workshop,* Utah, paper no . 86 , 9 –12 Aug 1998 .

[20] P. P. Vaidyanathan and P-Q Hoang, "Lattice structures for optimal design and robust implementation of two-channel perfect reconstruction QMF banks",

IEEE Trans. on ASSP, Jan 1988, pp 81-94.

[21] N. G. Kingsbury, "Matlab codes for design of Q-shift Complex Wavelet," http://sigproc.eng.cam.ac.uk/Main/NGK.

[22] R. Yu, "A new shift-invariance of discrete-time systems and its application to discrete wavelet transform analysis," *IEEE Trans. Signal Process.*, vol. 57, pp. 2527–2537, Jul. 2009.